Human Pathology (2021) **107**, 69–79

ELSEVIER

Human PATHOLOGY

www.elsevier.com/locate/humpath

Original contribution

Loss of SFRP1 expression is a key progression event in gastrointestinal stromal tumor pathogenesis☆,☆☆

Cher-Wei Liang MD [a,b,c], Ching-Yao Yang MD, PhD [d], Richard Flavin MD [e], Jonathan A. Fletcher MD [f], Tzu-Pin Lu PhD [g], I-Rue Lai MD, PhD [d], Yu-I Li MD, PhD [b], Yih-Leong Chang MD [a,], Jen-Chieh Lee MD, PhD [a,*]**

[a] *Department and Graduate Institute of Pathology, National Taiwan University Hospital and National Taiwan University College of Medicine, Taipei, 10002, Taiwan*
[b] *Department of Pathology, Fu Jen Catholic University Hospital, Fu Jen Catholic University, New Taipei City, 24352, Taiwan*
[c] *School of Medicine, College of Medicine, Fu Jen Catholic University, New Taipei City, 24205, Taiwan*
[d] *Department of Surgery, National Taiwan University Hospital and National Taiwan University College of Medicine, Taipei, 10002, Taiwan*
[e] *Department of Pathology, St. James's Hospital and Trinity College Dublin, Dublin, D02, Ireland*
[f] *Department of Pathology, Brigham and Women's Hospital and Harvard Medical School, Boston, MA, 02115, USA*
[g] *Department of Public Health, Institute of Epidemiology and Preventive Medicine, National Taiwan University, Taipei, 10055, Taiwan*

Received 30 August 2020; revised 26 October 2020; accepted 30 October 2020

Available online 10 November 2020

Keywords:
Gastrointestinal stromal tumor;
SFRP1;
CDKN2A;

Summary The mechanism of high-grade transformation in gastrointestinal stromal tumors (GISTs) remains to be clarified. We aim to discover the key progression events by studying biphasic GISTs. The study group included 101 GISTs. Nineteen of these had been screened from 263 GISTs to represent the early stage of GIST high-grade transformation, characterized by juxtaposed low-grade and high-grade regions in the same tumor (so-called biphasic GISTs). Mutational analyses, fluorescence in situ

Abbreviations: ALT, alternative lengthening of telomere; EZH2, enhancer of zeste 2 polycomb repressive complex 2 subunit; FISH, fluorescence in situ hybridization; FFPE, formalin-fixed paraffin-embedded; GIST, gastrointestinal stromal tumor; H3K27, Lys-27 of histone H3; IHC, immunohistochemistry; PCR, polymerase chain reaction; RTK, receptor tyrosine kinase; SFRP, secreted frizzled-related protein; TKI, tyrosine kinase inhibitor.

☆ Competing interest: The authors declare no potential conflict.

☆☆ Funding: This work was supported by the Ministry of Science and Technology, Taiwan [grant numbers NSC102-2320-B-002] Cathay General Hospital, Taiwan [grant number CGH-MR-10005].

* Corresponding author. Department and Graduate Institute of Pathology, National Taiwan University Hospital and National Taiwan University College of Medicine, 7 Chung-Shan South Road, Taipei, 10002, Taiwan.

** Corresponding author. Department and Graduate, Institute of Pathology, National Taiwan University Hospital and National Taiwan University College of Medicine, 7 Chung-Shan South Road, Taipei, 10002, Taiwan.

E-mail addresses: ntuhylc@gmail.com (Y.-L. Chang), leejenchieh@ntuh.gov.tw (J.-C. Lee).

https://doi.org/10.1016/j.humpath.2020.10.010
0046-8177/© 2020 Elsevier Inc. All rights reserved.

p16(INK4a);
NanoString

hybridization (FISH), NanoString analyses, telomere analysis, and gene expression profiling were carried out, followed by *in silico* analyses, cell line study, and immunohistochemical validation. Using gene expression analysis, downregulation of *SFRP1* was revealed to be the main event in GIST high-grade transformation ($p = 0.013$), accompanied by upregulation of *EZH2*. *In silico* analyses revealed that downregulation of *SFRP1* was a common feature in GIST progression across several different series. Immunohistochemically, the expression of SFRP1 was validated to be significantly lower in high-grade GISTs (WHO risk group 3a or higher) than in low-grade GISTs ($p < 0.001$), and attenuation/loss of SFRP1 was associated with GIST tumor progression ($p < 0.001$). By NanoString and FISH analyses, chromosomal 9/9p loss was the only recurrent large-scale chromosome aberration in biphasic GISTs, with a correlation with SFRP1 downregulation. Subclones containing chromosome 9/9p loss could be appreciated in the low-grade parts of biphasic GISTs. *TP53* mutation, *RB1* loss, *KIT/PDGFRA* mutation, and alternative lengthening of telomeres did not play a significant role in GIST high-grade transformation. In conclusion, high-grade transformation of GISTs features *SFRP1* downregulation and chromosome 9/9p loss.
© 2020 Elsevier Inc. All rights reserved.

1. Introduction

Gastrointestinal stromal tumor (GIST), the most common mesenchymal tumor of the gastrointestinal tract, represents a compelling model in which to characterize early oncogenic progression in sarcoma. Our current knowledge indicates stepwise tumor progression in GISTs. The earliest event is a gain-of-function mutation in the *KIT/PDGFRA* gene, leading to constitutive activation of the corresponding receptor tyrosine kinase (RTK) proteins in more than 85% of GISTs [1−3]. This is the basis for current RTK-targeted therapies [1,2]. The formation and growth of microGISTs (defined as subclinical GISTs less than 1.0 cm in diameter) then ensues, which entails the cooperation of additional genetic alterations [4−6]. However, this genetic progression in microGISTs is often thwarted by tumor involution [4−6].

When microGISTs do occasionally succeed in progression to larger clinical GISTs, the clonal evolution results from accumulation of cytogenetic abnormalities in distinct profiles. The early changes usually include monosomy 14, monosomy 22, and 1p deletion [7−10]. This is accompanied by MYC-associated factor X (*MAX*) gene inactivating mutation [5] followed by 9p deletion, targeting the tumor suppressor gene *CDKN2A*, which encodes p16 and p14 proteins, and which appears to be a crucial factor in GIST progression [8−11]. Concurrent with p16 dysregulation, or thereafter, late events occur, which include the downregulation of *DMD* (which encodes dystrophin) [12]. After tyrosine kinase inhibitor (TKI) treatment, additional genetic changes culminate in the emergence and dominance of resistant subclones [13].

However, the biologic mechanisms of GIST high-grade transformation are not well characterized. Previous studies regarding this issue mostly focused on tumor groups at the two ends of development, where the initial events responsible for high-grade transformation either had yet to occur or had been obscured by subsequent genetic changes during tumor progression [8−11]. To better define the transitional aberrations, we aimed to study GIST specimens containing discrete concurrent low-grade and high-grade aspects (hereafter referred to as biphasic GISTs). Our goal was to characterize genetic changes that initiate the high-grade transformation (Fig. 1). To this end, we evaluated gene expression profiles, large-scale chromosomal aberrations, intratumoral heterogeneity, and immunohistochemistry (IHC) in low-grade *vs.* high-grade regions of the same GISTs. Our findings suggest that downregulation of *SFRP1* and genetic instability of *CDKN2A* play important roles in GIST high-grade transformation.

2. Materials and methods

2.1. Tumor collection

We retrospectively screened archived GIST specimens for biphasic GISTs. These GISTs were defined as GISTs harboring two morphologically distinct populations of neoplastic cells that had evident differences in cellularity, nuclear grade, and mitotic activity by ≥ 3 per 5 mm^2. A total of 263 GISTs were screened, which included 19 biphasic GISTs. Cases in which the differences were caused by tumor regression or subclonal progression after sarcomatous change of the whole tumors were excluded. In each biphasic GIST, tissue sections containing juxtaposed low-grade and high-grade regions were selected for further studies. Additional 82 cases of conventional GISTs without biphasic component were included for immunohistochemical and fluorescence in situ hybridization (FISH) validation, including 46 cases of WHO risk groups 1/2 and 36 cases of risk groups greater than 3a.

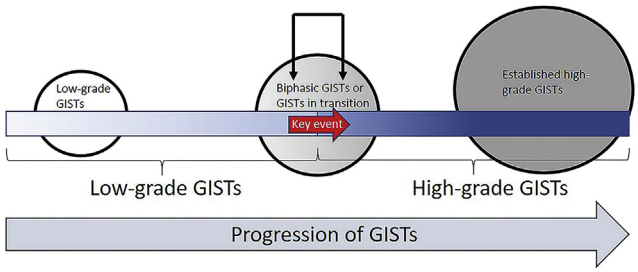

Fig. 1 An illustration of the project concept. Biphasic GISTs are low-grade GISTs in evolution to a higher grade tumor (tumors in transition). Studying biphasic GISTs has the advantage that background pathological and technical confounding factors are minimized, such as differences in gene expression between individual tumors, different tumor location, alternate tumor stages, different specimen storage time, and processing times. GISTs, gastrointestinal stromal tumors.

The study was approved by the Institutional Review Board of National Taiwan University Hospital (REC No.: 201212067RIND).

2.2. Mutational analysis

In each biphasic GIST, selected low-grade areas, high-grade areas, and normal smooth muscle areas (as control) were manually microdissected. DNA was extracted with the QIAamp® DNA FFPE Kit (Qiagen, Valencia, USA) and RNA with the RecoverAll™ Kit FFPE (Life Technologies, Taipei, Taiwan). *KIT* exons 9/11/13/17, *PDGFRA* exons 12/14/18, and *TP53* exons 5–9 were Sanger sequenced [6,14].

2.3. Large-scale genetic aberrations and gene expression profiling

The NanoString nCounter™ Human Cancer Reference and Human Karyotype Kit were used for detecting large-scale chromosomal changes, and nCounterTM PanCancer Pathway Panel was used for gene expression profiling (GEP). The copy number alterations were displayed by Integrative Genomic Viewer. If a copy number alteration occurred in at least 3 cases, it was defined as a frequently recurrent event. The GEP data were quantile normalized by R and analyzed by Partek® Genomics Suite (Partek Inc., St. Louis, MO, USA). NanoString nSolver 2.0 software was used to reveal differentially expressed (DE) genes in low-grade-high-grade tumor pairs. The functional analyses were analyzed by Ingenuity Pathway Analysis (IPA, QIAGEN). *In silico* analyses of open GIST microarray data sets (GSE20710/GSE8167/GSE31802) were performed. More details are provided in Supplemental Methods.

2.4. IHC, FISH), and alternative lengthening of telomeres

Four-micron-thick formalin-fixed-paraffin-embedded tissue sections were used for IHC validation. The primary antibodies and methods used are detailed in Supplemental Table 1. *CDKN2A* FISH validation was performed on representative low-grade and high-grade regions. Additional probes used in further validation included chromosomes 10/11/13/14/17/18/22 DNA probes (Supplemental Methods) and a telomere-specific PNA probe for alternative lengthening of telomeres (ALTs) [15].

3. Results

3.1. Clinicopathological features of biphasic GISTs

A total of 263 GISTs were screened, which included 19 biphasic GISTs (7.2%) (Fig. 2A). The clinicopathological features are detailed in Supplemental Table 2, 3, and 4. In all tumors, both low-grade and high-grade regions shared the same *KIT/PDGFRA* mutation. Histologically, tumor progression was characterized by an increase in cellularity, nuclear size, and mitotic activity, paralleling an increase in Ki-67 proliferative activity (Fig. 2B and C).

3.2. Chromosomal 9/9p loss was the only frequently recurrent event in high-grade transformation of biphasic GISTs

Fifteen biphasic GISTs were interrogated by NanoString nCounter™ analysis. The high-grade parts showed additional chromosomal aberrations when compared with the corresponding low-grade regions (Fig. 3, Supplemental Data 1, Supplemental Table 3). Losses of chromosome 14q (60%), 22q (35.7%), and 1p (8/15 = 53.3%) were the most common events in the original low-grade regions. Chromosome 9/9p loss, found in 8 cases (53.3%), was the only frequently recurrent event detected in high-grade transformation. In the 4 cases not available for NanoString analysis, one also showed *CDKN2A* deletion by FISH, suggesting chromosome 9/9p loss (total 9/19 = 47.4%; 5 heterozygous, 4 homozygous, $p = 0.003$). Chromosome 9/9p loss was the sole large-scale event in 2 cases (2/8 = 25%). In another 2 cases, chromosome 9/9p loss was detected in both low- and high-grade regions. Supplemental Table 3 provides a summary of 9/9p status in each case. Other large-scale chromosomal changes found in high-grade transformation were 17p gain (13.3%), 11q loss (13.3%), and 13q loss (13.3%). No difference in gender, tumor size, location, mitotic counts, or Ki-67 proliferative index was found between cases with and without 9/9p loss in the high-grade regions. By FISH validation, *CDKN2A*-deleted subclones could be detected in the low-grade parts

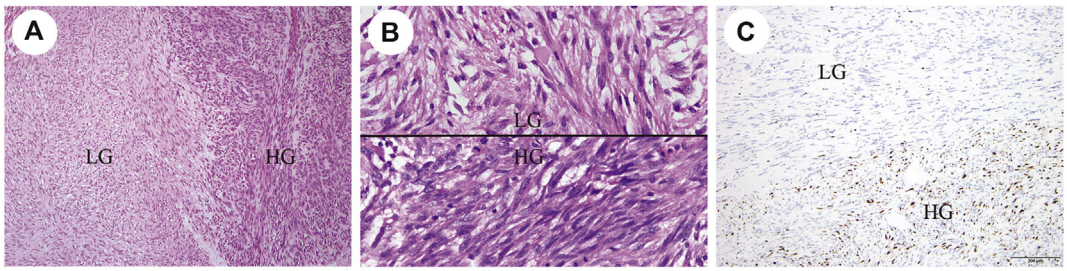

Fig. 2 (A) GISTs that contained juxtaposed low-grade (LG) and high-grade (HG) regions on the same slide (100 ×), so-called *biphasic* GISTs. (B) Histologically, the tumor progression was characterized by an increase in cellularity, nuclear size, and mitotic activity. Upper panel: low-grade part; lower panel: high-grade part (400×). (C) Differential Ki-67 proliferative index in a biphasic GIST (100×). GISTs, gastrointestinal stromal tumors.

of biphasic GISTs but not in purely low-grade GISTs (Supplemental Data 2), suggesting genetic instability in biphasic GISTs.

3.3. Downregulation of SFRP1 expression was a key progression factor revealed by GEP (GEO GSE75479) and a common event in GIST progression across different series

Six biphasic GISTs with paired low-grade and high-grade regions were analyzed by NanoString GEP system (see Supplemental Fig. 1 for platform adequacy validation). Important genes were selected by $mFDR_{min}$ across samples [16]. Downregulation of *SFRP1* and upregulation of *EZH2* were recurrent events found in more than 3 analytical methods across all cases (Fig. 4A–D). IPA analysis revealed that *SFRP1* downregulation was associated with histone modification and the MYC pathway. *In silico* analyses revealed that downregulation of *SFRP1* expression (nonparametric Wilcoxon rank sum test, GEO GSE8167, $p < 0.0001$; GSE20710, $p = 0.025$; GSE31802, $p = 0.0303$) (Fig. 5A–C), as well as upregulation of *EZH2* ($p < 0.05$) (Fig. 5D–F), was a common feature in GIST progression

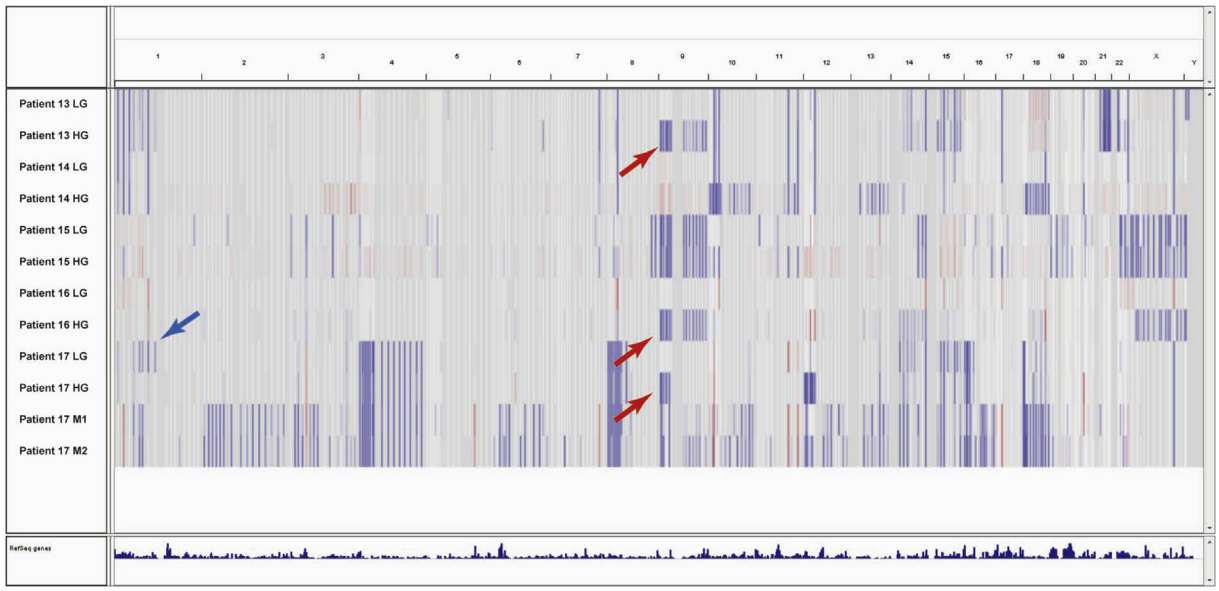

Fig. 3 Large-scale chromosomal variations in *biphasic* GISTs by NanoString nCounter™ analysis. Selected cases are shown (cases 13–17). Chromosome 9/9p losses are indicated by red arrows. In patient 13, chromosome 9 loss was one of the very few large-scale changes in high-grade transformation. In patient 17, two metastatic lesions (M1 and M2) were also included for comparison. Note that in the metastatic lesions, there were more additional aberrations, which made impossible the direct comparison between metastatic and primary tumors for detection of early changes in tumor progression. This highlighted the importance of studying biphasic GISTs, where the very early changes were possibly not masked. Also note that in the last patient, the low-grade part harbored chromosomal 1p loss (blue arrow), which was not found in the high-grade part. This may indicate that the high-grade part of the tumor was derived from a subclone of cells in the low-grade part. (For interpretation of the references to colour in this figure legend, the reader is referred to the Web version of this article.) GISTs, gastrointestinal stromal tumors.

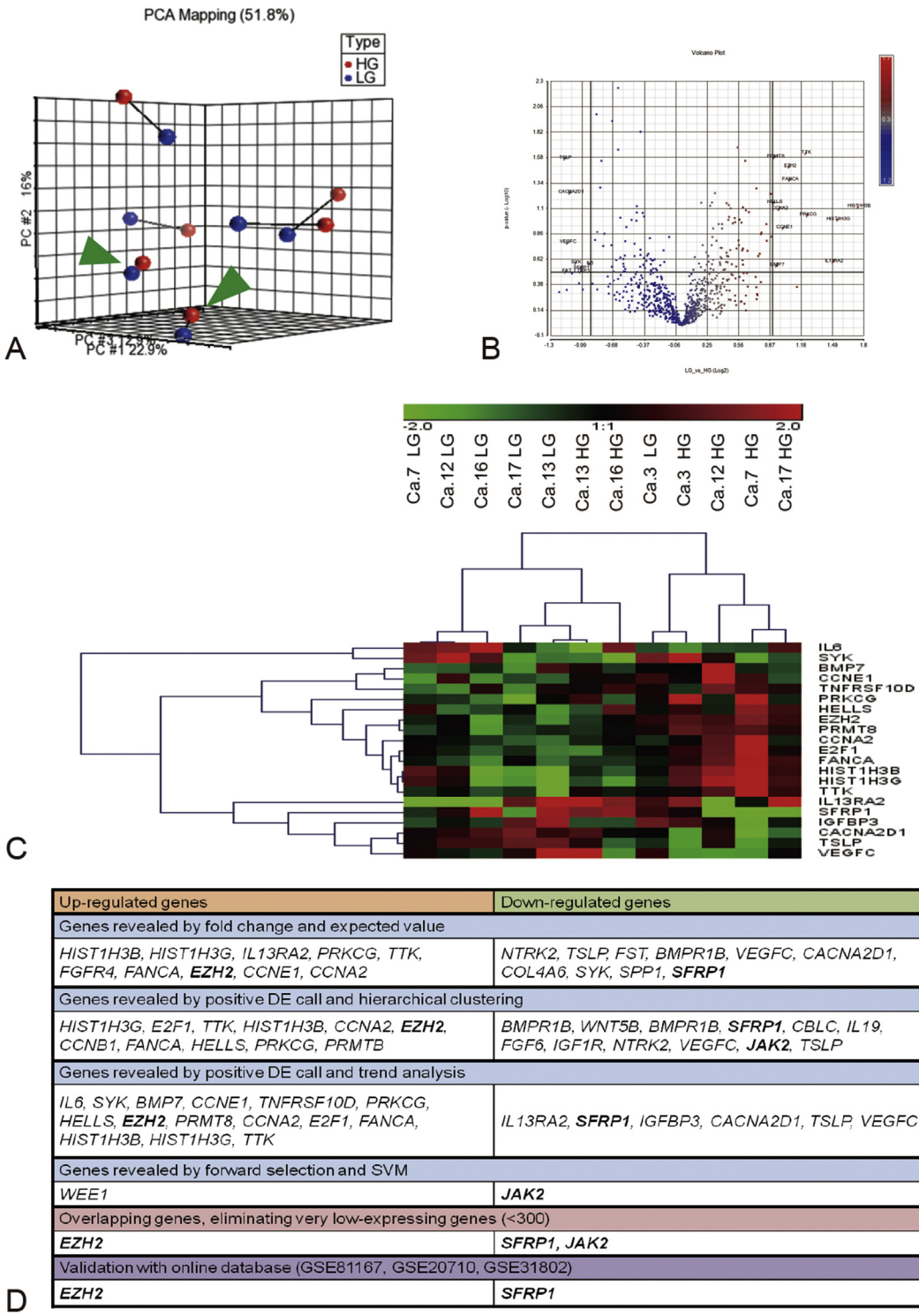

D

Up-regulated genes	Down-regulated genes
Genes revealed by fold change and expected value	
HIST1H3B, HIST1H3G, IL13RA2, PRKCG, TTK, FGFR4, FANCA, ***EZH2****, CCNE1, CCNA2*	*NTRK2, TSLP, FST, BMPR1B, VEGFC, CACNA2D1, COL4A6, SYK, SPP1,* ***SFRP1***
Genes revealed by positive DE call and hierarchical clustering	
HIST1H3G, E2F1, TTK, HIST1H3B, CCNA2, ***EZH2****, CCNB1, FANCA, HELLS, PRKCG, PRMTB*	*BMPR1B, WNT5B, BMPR1B,* ***SFRP1****, CBLC, IL19, FGF6, IGF1R, NTRK2, VEGFC,* ***JAK2****, TSLP*
Genes revealed by positive DE call and trend analysis	
IL6, SYK, BMP7, CCNE1, TNFRSF10D, PRKCG, HELLS, ***EZH2****, PRMT8, CCNA2, E2F1, FANCA, HIST1H3B, HIST1H3G, TTK*	*IL13RA2,* ***SFRP1****, IGFBP3, CACNA2D1, TSLP, VEGFC*
Genes revealed by forward selection and SVM	
WEE1	***JAK2***
Overlapping genes, eliminating very low-expressing genes (<300)	
EZH2	***SFRP1, JAK2***
Validation with online database (GSE81167, GSE20710, GSE31802)	
EZH2	***SFRP1***

Fig. 4 Gene expression profiles in biphasic GISTs. (A) Principle component analysis (PCA). Red spheres: high-grade regions. Blue spheres: low-grade regions. Profiles from the same tumor were linked by a black line. There were 2 cases (patients 3 and 13) where the two intratumoral parts were very similar to each other; these were the two cases that had very few large-scale events other than 9/9p loss in high-grade transformation (green arrowhead). (B) Volcano plot. Significant genes ($p < 0.05$) in high-grade transformation were revealed by fold changes. (C) Supervised hierarchical clustering by genes revealed by positive DE call. Relevant upregulated and downregulated genes were revealed. Note that in patients 3 and 13, the two parts clustered together, as revealed by PCA. (D) Upregulated and downregulated genes revealed by different analytical methods (see text). Only *SFRP1* and *EZH2* were revealed recurrently by different methods after *in silico* validation and filtering out very low-expressing genes. (For interpretation of the references to scolour in this figure legend, the reader is referred to the Web version of this article.) GISTs, gastrointestinal stromal tumors.

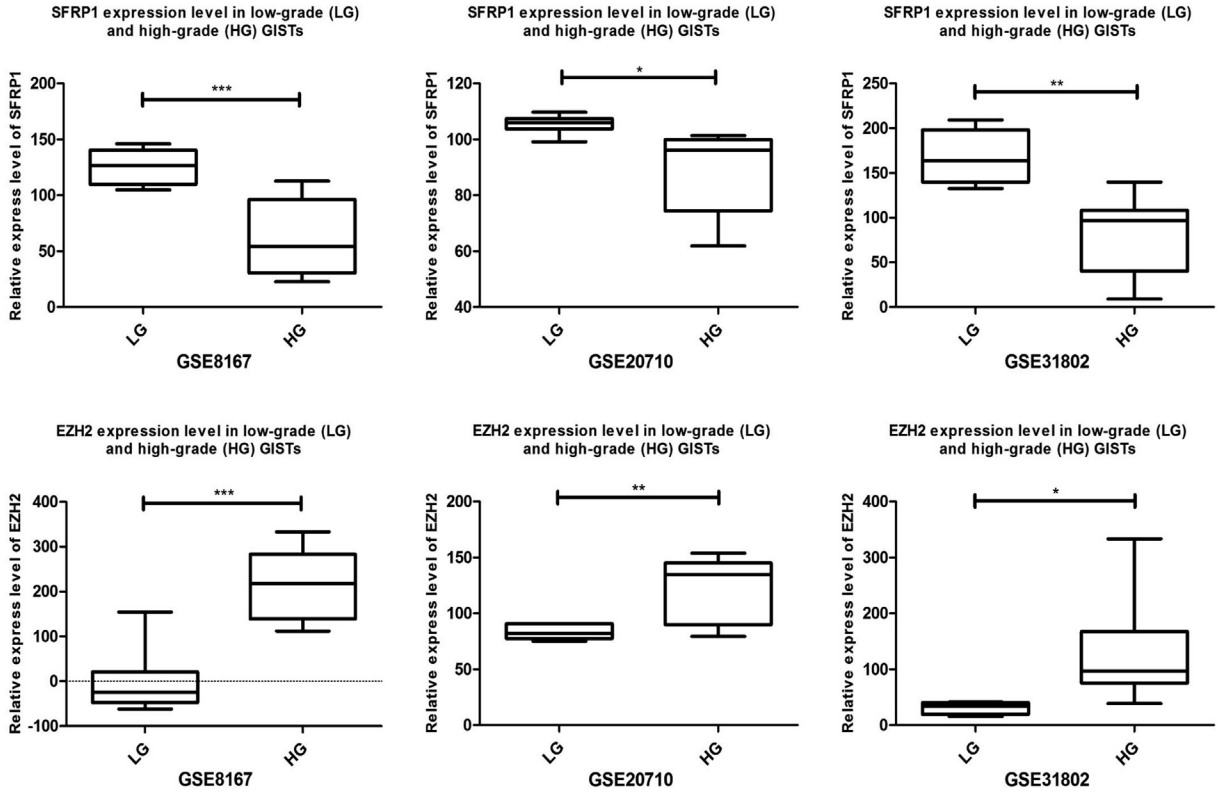

Fig. 5 By gene expression profiles, *in silico* analyses of online data sets revealed that downregulation of *SFRP1* expression (A–C) and upregulation of *EZH2* (D–F) in GIST progression were common features across several different series (GEO GSE8167, GSE20710, GSE31802; $p < 0.05$), in which full-blown high-grade GISTs were compared with low-grade ones (box plots). GISTs, gastrointestinal stromal tumors.

across several different series [7,17]. Results of cell line validation are provided in Supplemental Fig. 2.

3.4. Validation of SFRP1 and p16 expression by IHC

In biphasic GISTs, the immunoreactivity to SFRP1 was significantly lower in the high-grade region (paired *t*, $p = 0.013$) (Fig. 6A–C, Supplemental Table 4). In additional GIST cases, the immunostaining for SFRP1 in low-risk GISTs showed diffuse and strong staining and was a general finding across spindle/epithelioid cases (Fig. 6D–G). When GISTs increased in size, the staining tended to decrease in intensity (Fig. 6D and H-J). Occasionally, a Golgi pattern could be observed (Fig. 6I). In sarcomatous GISTs, loss of SFRP1 staining was a common finding (Fig. 6J). The expression of SFRP1 was significantly lower (Mann-Whitney rank test, $p < 0.001$) in higher grade GISTs (risk groups 3a or greater) than in lower grade GISTs (risk groups 1/2) (Fig. 7AB). Trend analysis showed that the higher the GIST risk, the lower the SFRP1 expression (*Chi* square trend, $p < 0.001$) (Fig. 7C). The expression of SFRP1 showed a reverse correlation with tumor size (linear regression, $R^2 = 0.1559$, $p = 0.0002$), a reverse trend with mitotic counts ($R^2 = 0.044$, $p = 0.058$), but no correlation with patient gender, age, *KIT* mutational loci, or tumor location. The downregulation of SFRP1 expression was significantly associated with *KIT/PDGFRA*-mutated GISTs with 9/9p loss (Fig. 7D, $p = 0.035$) and not significantly with cases without 9/9p loss (Fig. 7E, $p = 0.09$). *In silico* analysis revealed the same trend by GEP. While the correlation between p16 IHC staining and *CDKN2A* gene status was not constant (Supplemental Table 5), there was a weak reciprocal correlation between the p16 and SFRP1 IHC staining intensities ($r = -0.303$, $p = 0.072$, Fig. 7F and G). SFRP1 (8p11) downregulation was not associated with large-scale chromosome 8p change or other chromosomal aberrations. SFRP1 expression did not correlate with MAX expression (Supplemental Table 4).

3.5. No TP53 mutation or ALTs

No TP53 mutation or ALT was detected in biphasic GISTs as previously reported [15,18]. In addition, no ATRX loss was noted by IHC.

4. Discussion

Establishing a sarcoma progression model is crucial in seeking opportunities in sarcoma management. However,

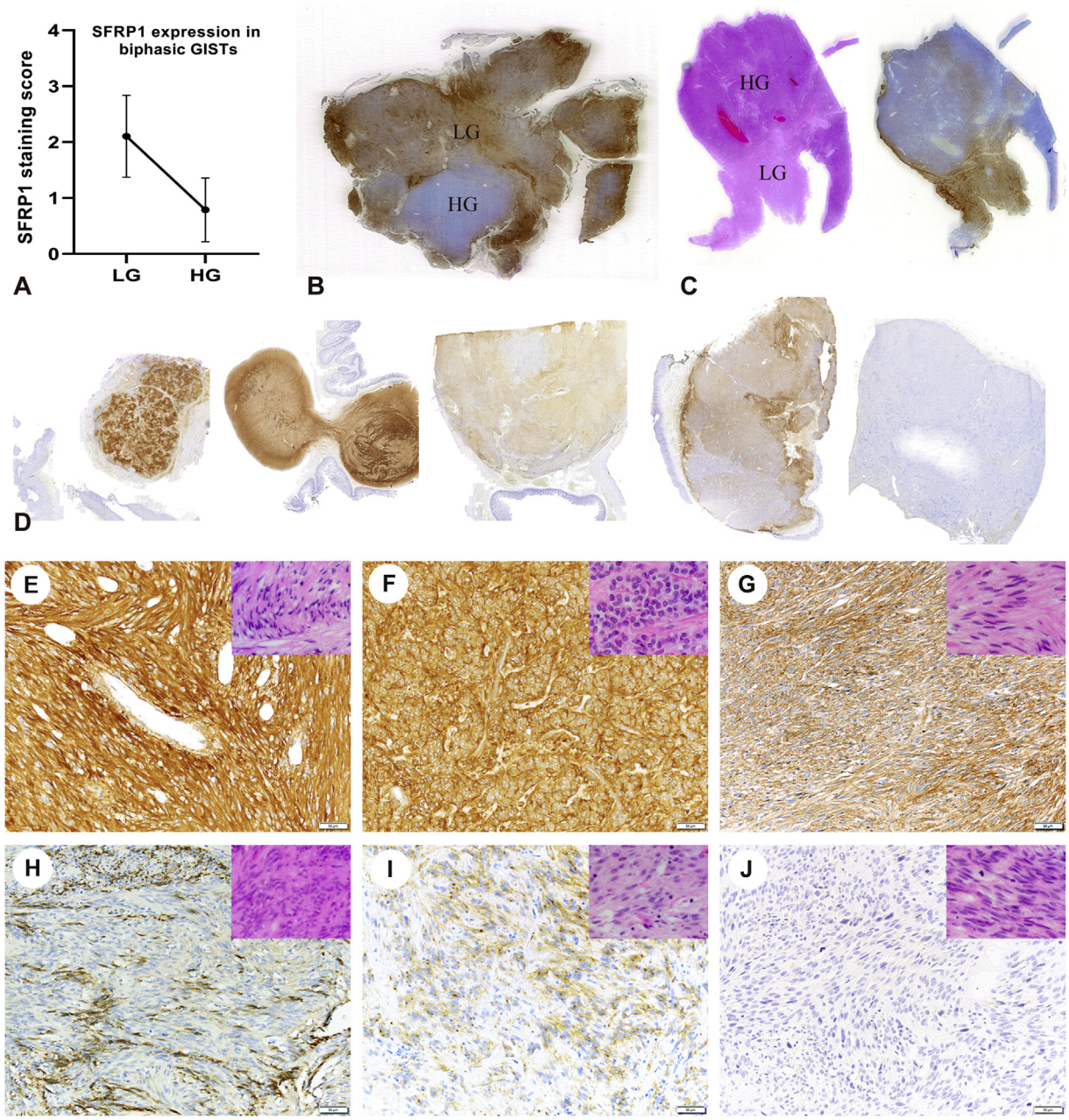

Fig. 6 (A–C) Validation of SFRP1 expression in biphasic GISTs by immunohistochemistry. (A) Immunohistochemically, the expression of SFRP1 was significantly lower in the high-grade regions than in the low-grade regions in biphasic GISTs (paired t, $p = 0.013$). (B) A PDGFRA-mutated (D842V) gastric case with heterozygous 9p loss showed loss of SFRP1 protein expression in the high-grade region. (C) A KIT-mutated (W557_V559delinsC) duodenal case with heterozygous 9p loss showed marked reduction in SFRP1 protein expression in the high-grade region. (E–J) Validation of SFRP1 expression in additional conventional GIST samples. (D) The staining of SFRP1 was clear cut and usually could be easily visualized under lower power magnification. When GISTs increased in size, the staining was usually attenuated or lost. From left to right: WHO risk group 1 (1.5 cm), 2 (2.5 cm), 2 (3.8 cm), 3a (6.3 cm), 6 b (13.0 cm). (E) A low-grade spindle GIST stained diffusely and strongly for SFRP1 (200×). The stain pattern was cytoplasmic, membranous, and interstitial. (F) A low-grade epithelioid GIST stained diffusely and strongly for SFRP1 (200×). When GISTs progressed, the SFRP1 staining usually decreased, either in a diffusely attenuated pattern (G) or in a multiple-patch loss pattern (H) (200×). (I) Occasionally, the attenuated staining showed a Golgi pattern (200×). (J) Loss of SFRP1 staining was a common finding in sarcomatous GISTs (200×). The corresponding H&E images are shown as insets (400×). GISTs, gastrointestinal stromal tumors.

study of early sarcoma progression is extremely difficult owing to the lack of adequate tumor samples. Our previous study has shown that the losses of chromosome 14, 22, and 1p are common events (GEO GSE28469) in benign

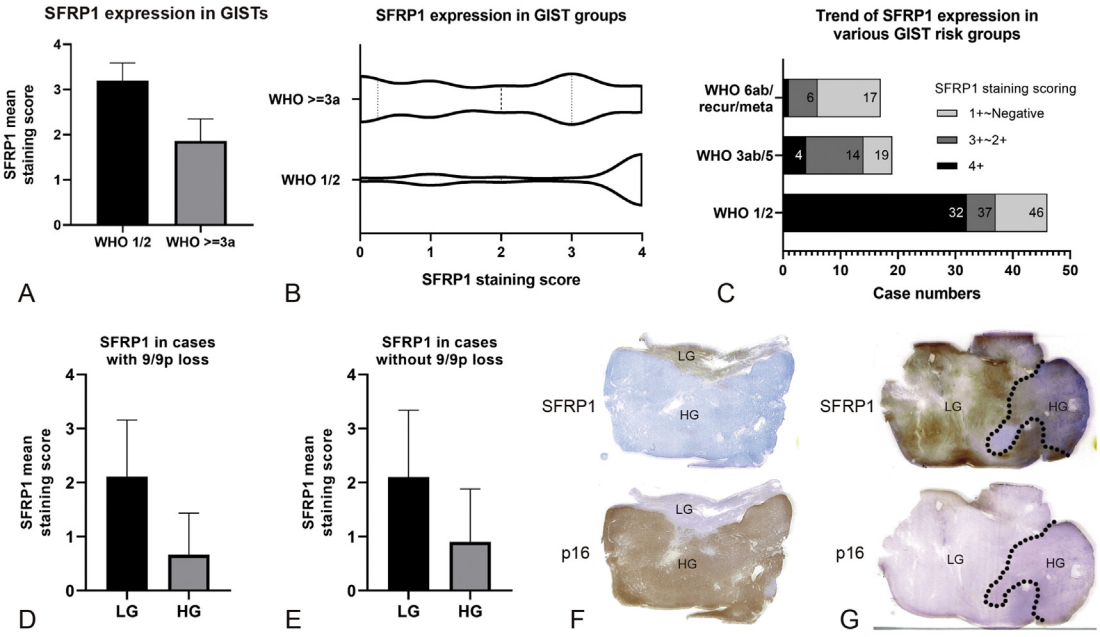

Fig. 7 (A–C) Trend analysis of SFRP1 expression in additional conventional GIST samples. (A) Immunohistochemically, the mean expression level of SFRP1 was significantly lower in higher grade GISTs than in lower grade GISTs (WHO risk group 1/2). (B) A violin plot showing SFRP1 expression in various GIST groups. The expression of SFRP1 usually started to decrease when a GIST reached WHO risk group 3a. (C) Trend analysis showed the trend of SFRP1 downregulation in higher risk GISTs. (D–G) The correlation between SFRP1 expression and chromosome 9/9p loss. (D) The downregulation of SFRP1 expression was associated with *KIT/PDGFRA* mutated GISTs with 9/9p loss ($p = 0.035$) but (E) not with cases without 9/9p loss ($p = 0.09$). However, the significance was only marginal and it is difficult to make a conclusion. Reduction in SFRP1 expression was a consistent feature in cases with chromosome 9/9p loss but p16 expression varied. (F) A heterozygous *CDKN2A*-deleted case showed p16 staining in the high-grade region, imparting an inverse mirror image with the SFRP1 staining. There was a weak reciprocal correlation between the p16 and the SFRP1 staining intensities across all the samples ($r = -0.303$, $p = 0.072$), indicating a possible interaction between the two. (G) Another case with heterozygous chromosome 9 loss showed no p16 staining in both parts of the tumor. Reduction in SFRP1 staining in the high-grade region was still appreciated. GISTs, gastrointestinal stromal tumors.

microGISTs and are unlikely to be the initiation events in high-grade tumor transformation [4,5]. Losses of chromosomes 10 and 15 and gain of chromosome 5 are also occasionally seen in microGISTs, arguing against their roles as the sole event in high-grade transformation [4]. Loss of 9p is the most convincing chromosomal abnormality that may play a role in high-grade transformation based on several previous studies [8–11]. However, most of these studies have focused on tumor groups from different patients, specifically analyzing discrete points in GIST tumor progression (*i.e.*, low-grade *vs.* well-established high-grade tumors). To narrow down the scope of surveillance and minimize confounding factors, we chose to study *biphasic* GISTs that captured the key stage of tumor progression within the same tumor.

In 2009, Agaimy et al. [19] studied six biphasic GISTs and revealed their divergent molecular cytogenetic progression. In that study, most of the so-called biphasic tumors represented focal tumor regression or intratumoral subclonal progression from an already high-grade sarcomatous tumors, and only two cases fulfilled the criteria proposed here. Of these two cases, none revealed chromosome 9 loss in the high-grade region of the primary tumors; however, in one case, chromosome 9 loss was detected in the metastatic tumor. The result suggested that chromosome 9 loss might be a relatively late rather than early event in high-grade transformation. By contrast, in our series, we found chromosome 9/9p loss to be the only frequently recurrent event in high-grade progression. *CDKN2A* is a key tumor suppressor on chromosome 9p and regulates cell cycle progression. Because *CDKN2A* mutation was only found in high-grade GISTs, it is reasonable to postulate that after a low-grade GIST acquires deleterious *CDKN2A* mutation, with loss of cell cycle control, the involved tumor cells proliferate rapidly, thereby evolving into a high-grade tumor. We took advantage of 5-μm section FISH to gain a topographical view of *CDKN2A* intratumoral heterogeneity. We found that even in the low-grade region of biphasic GISTs, there were already subclones that showed heterozygous *CDKN2A* loss. This subclonal diversity was not observed in usual low-grade GISTs (Supplemental Data 2) and thus indicates that *CDKN2A* genetic instability may play a role in GIST transformation. Although homozygous *CDKN2A* deletion could be

consistently reflected by IHC showing complete loss of p16 protein staining, cases with heterozygous or no *CDKN2A* deletion might demonstrate p16 expression in varying degrees, limiting the usage of immunostaining as a surrogate in practice. In fact, p16 protein expression is associated with *CDKN2A* mutation, promoter methylation, enhanced transcription, or other alterations and may reflect a mechanism that counteracts senescence caused by rapid cell proliferation, even in cases with single copy loss of *CDKN2A* [20,21].

By studying biphasic GISTs, we also demonstrate that *SFRP1* downregulation is a key factor in GIST transformation. *SFRP1* encodes a member of the secreted frizzled-related protein family that impedes the Wnt signaling pathway [22,23]. *SFRP1* is a highly expressed tumor suppressor gene in microGISTs (GEO GSE28469) and low-grade GISTs, and its downregulation is a consistent feature among high-grade tumors [7,17]. The reduction does not appear to be related to gene dosage or mutation, as revealed by previous chromosome studies and whole genome/exome sequencing [24–27]. An epigenetic event is the most likely explanation [22]. Interestingly, downregulation of *SFRP1* is also found in malignant progression of gastrointestinal epithelial tumors [28–33], implying that tumor location may play a role in tumor progression models.

In addition to *SFRP1* downregulation, we also found upregulation of *EZH2*, which is a key protein of the polycomb family and can methylate Lys-27 of histone H3 leading to transcriptional repression of target genes. Because promoter methylation is a rare event in *SFRP1* in GISTs [34], it is rational to hypothesize that the repressive histone modification by EZH2 might contribute to *SFRP1* downregulation.

By IPA analysis, the reduction in SFRP1 level was associated with the MYC pathway, which has been demonstrated to participate in high-grade transformation of GISTs [5]. However, MYC is usually not overexpressed by IHC in GISTs until the very late stage [5]. This is not unexpected because the usual positive MYC immunohistochemical reference point is in cancers harboring *MYC* gene amplification, which is a rare event in GISTs [5]. Interestingly, in parallel, *MAX*, which forms a heterodimer with MYC/MAD as a transcriptional activator/repressor, is located on chromosome 14, whose loss is the most common cytogenetic event in small GISTs [5]. Inactivating mutation in the *MAX* gene is also prevalent in a subset of small GISTs, emphasizing the role of MAX loss in early GIST progression. In the present study, most biphasic GISTs showed attenuated MAX staining in both parts of the tumors (Supplemental Table 4), indicating that MAX inactivation usually occurs ahead of SFRP1 downregulation.

The limitation of the present study is the lack of functional validation, in part owing to the lack of appropriate materials from small GISTs. Further studies are required to clarify the potential interplay between SFRP1, KIT/PDGFRA, and p16(INK4a) in GIST progression. We tried to correlate the loss of *CDKN2A* on FISH slide with attenuation of SFRP1 expression on immunohistochemical slide but unfortunately failed because a proper image alignment tool is lacking. By IHC, attenuation of SFRP1 staining showed a trend toward association with p16 overexpression, which, however, was not a constant finding. In search of literature including open databases of proteins and genome, no data of confirmed interaction between KIT/PDGFRA, SFRP1, and p16 (*CDKN2A*) could be found. However, similar findings of simultaneous SFRP1 and p16 downregulation in tumor progression have been reported in

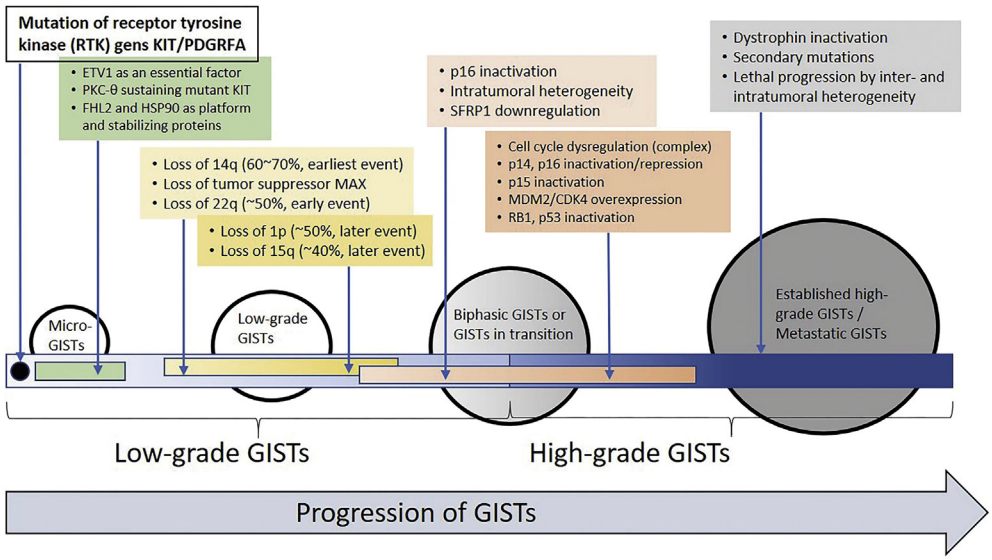

Fig. 8 Summary of progression events in GISTs. The model applies to adult sporadic type GISTs. The progression events in pediatric GISTs, SDH-deficient GISTs, and quadruple-negative GISTs are not depicted. GISTs, gastrointestinal stromal tumors; SDH, succinate dehydrogenase.

colorectal cancer, hepatocellular carcinoma, and nonsmall-cell lung cancer [35−37]. It has been postulated that during tumor progression, a general epigenetic methylation process occurs, resulting in hypermethylation of several important tumor suppressor genes including *CDKN2A* and *SFRP1*, to promote cancer aggressiveness [35−37]. In one study, colony formation assay of two lung cancer cell lines was performed, and reduction of colony formation with *SFRP1* transfection was found, proving the tumor suppressor role of SFRP1 [37].

In conclusion, by studying biphasic GISTs, we demonstrate that downregulation of SFRP1 and chromosome 9/9p loss are major events in GIST high-grade transformation. These results could help to refine GIST progression models and provide biomarkers for the design of individualized therapies. The proposed model of progression events in GISTs is summarized in Fig. 8.

Transcript profiling

GEP data of this study have been submitted to the Gene Expression Omnibus database (accession number GSE 75479). http://www.ncbi.nlm.nih.gov/geo/query/acc.cgi?acc=GSE75479.

Appendix A. Supplementary data

Supplementary data to this article can be found online at https://doi.org/10.1016/j.humpath.2020.10.010.supportedgrants

Acknowledgments

C.-W.L. contributed in conceptualization, data curation, formal analysis, funding acquisition, investigation, methodology, resources, software, validation, visualization, roles/writing the original draft for the study. C.-Y.Y. contributed in investigation, methodology, and resources for the study. R.F. contributed in investigation, data curation, visualization, and writing, reviewing, and editing for the study. J.A.F. contributed in methodology, resources, visualization, and writing, reviewing, and editing for the study. T.-P.L. contributed in formal analysis, methodology, resources, and software for the study. I.-R.L. contributed in resources and visualization. Y.-I.L. contributed in data curation, formal analysis, and validation. Y.-L.C. contributed in funding acquisition, project administration, resources, supervision, and writing, reviewing, and editing for the study. J.-C.L. contributed in data curation, project administration, resources, supervision, validation, visualization, and writing, reviewing, and editing for the study. This work was supported by grants from the Ministry of Science and Technology, Taiwan (NSC102-2320-B-002, C.W.L) and Cathay General Hospital, Taiwan (CGH-MR-10005, C.W.L).

References

[1] Demetri GD, von Mehren M, Antonescu CR, DeMatteo RP, Ganjoo KN, Maki RG, et al. NCCN Task Force report: update on the management of patients with gastrointestinal stromal tumors. J Natl Compr Canc Netw 2010;8(Suppl 2:S1):41. quiz S42-4.

[2] Corless CL, Heinrich MC. Molecular pathobiology of gastrointestinal stromal sarcomas. Annu Rev Pathol 2008;3:557−86.

[3] Joensuu H, Vehtari A, Riihimaki J, Nishida T, Steigen SE, Brabec P, et al. Risk of recurrence of gastrointestinal stromal tumour after surgery: an analysis of pooled population-based cohorts. Lancet Oncol 2012;13:265−74.

[4] Liang CW, Rossi S, Dei Tos AP, Foo WC, Fletcher JA. MicroGIST genomic aberrations highlight early mechanisms in GIST pathogenesis. Mod Pathol 2010;23:23A.

[5] Schaefer IM, Wang Y, Liang CW, Bahri N, Quattrone A, Doyle L, et al. MAX inactivation is an early event in GIST development that regulates p16 and cell proliferation. Nat Commun 2017;8:14674.

[6] Rossi S, Gasparotto D, Toffolatti L, Pastrello C, Gallina G, Marzotto A, et al. Molecular and clinicopathologic characterization of gastrointestinal stromal tumors (GISTs) of small size. Am J Surg Pathol 2010;34:1480−91.

[7] Astolfi A, Nannini M, Pantaleo MA, Di Battista M, Heinrich MC, Santini D, et al. A molecular portrait of gastrointestinal stromal tumors: an integrative analysis of gene expression profiling and high-resolution genomic copy number. Lab Invest 2010;90:1285−94.

[8] Belinsky MG, Skorobogatko YV, Rink L, Pei J, Cai KQ, Vanderveer LA, et al. High density DNA array analysis reveals distinct genomic profiles in a subset of gastrointestinal stromal tumors. Genes Chromosomes Cancer 2009;48:886−96.

[9] Assamaki R, Sarlomo-Rikala M, Lopez-Guerrero JA, Lasota J, Andersson LC, Llombart-Bosch A, et al. Array comparative genomic hybridization analysis of chromosomal imbalances and their target genes in gastrointestinal stromal tumors. Genes Chromosomes Cancer 2007;46:564−76.

[10] Gunawan B, Bergmann F, Hoer J, Langer C, Schumpelick V, Becker H, et al. Biological and clinical significance of cytogenetic abnormalities in low-risk and high-risk gastrointestinal stromal tumors. Hum Pathol 2002;33:316−21.

[11] Sabah M, Cummins R, Leader M, Kay E. Altered expression of cell cycle regulatory proteins in gastrointestinal stromal tumors: markers with potential prognostic implications. Hum Pathol 2006;37:648−55.

[12] Wang Y, Marino-Enriquez A, Bennett RR, Zhu M, Shen Y, Eilers G, et al. Dystrophin is a tumor suppressor in human cancers with myogenic programs. Nat Genet 2014;46:601−6.

[13] Serrano C, Wang Y, Marino-Enriquez A, Lee JC, Ravegnini G, Morgan JA, et al. KRAS and KIT gatekeeper mutations confer polyclonal primary imatinib resistance in GI stromal tumors: relevance of concomitant phosphatidylinositol 3-kinase/AKT dysregulation. J Clin Oncol 2015;33:e93−6.

[14] Corless CL, McGreevey L, Haley A, Town A, Heinrich MC. KIT mutations are common in incidental gastrointestinal stromal tumors one centimeter or less in size. Am J Pathol 2002;160:1567−72.

[15] Liau JY, Lee JC, Tsai JH, Yang CY, Liu TL, Ke ZL, et al. Comprehensive screening of alternative lengthening of telomeres phenotype and loss of ATRX expression in sarcomas. Mod Pathol 2015;28:1545−54.

[16] Rhodes DR, Yu J, Shanker K, Deshpande N, Varambally R, Ghosh D, et al. Large-scale meta-analysis of cancer microarray data identifies common transcriptional profiles of neoplastic transformation and progression. Proc Natl Acad Sci USA 2004;101:9309−14.

[17] Yamaguchi U, Nakayama R, Honda K, Ichikawa H, Hasegawa T, Shitashige M, et al. Distinct gene expression-defined classes of gastrointestinal stromal tumor. J Clin Oncol 2008;26:4100−8.

[18] Romeo S, Debiec-Rychter M, Van Glabbeke M, Van Paassen H, Comite P, Van Eijk R, et al. European Organization for Research and

Treatment of Cancer Soft Tissue and Bone Sarcoma Group. Cell cycle/apoptosis molecule expression correlates with imatinib response in patients with advanced gastrointestinal stromal tumors. Clin Cancer Res 2009;15:4191−8.

[19] Agaimy A, Haller F, Gunawan B, Wunsch PH, Fuzesi L. Distinct biphasic histomorphological pattern in gastrointestinal stromal tumours (GISTs) with common primary mutations but divergent molecular cytogenetic progression. Histopathology 2009;54:295−302.

[20] Huang HY, Huang WW, Lin CN, Eng HL, Li SH, Li CF, et al. Immunohistochemical expression of p16INK4A, Ki-67, and Mcm2 proteins in gastrointestinal stromal tumors: prognostic implications and correlations with risk stratification of NIH consensus criteria. Ann Surg Oncol 2006;13:1633−44.

[21] Okamoto Y, Sawaki A, Ito S, Nishida T, Takahashi T, Toyota M, et al. Aberrant DNA methylation associated with aggressiveness of gastrointestinal stromal tumour. Gut 2012;61:392−401.

[22] Takeshima H, Wakabayashi M, Hattori N, Yamashita S, Ushijima T. Identification of coexistence of DNA methylation and H3K27me3 specifically in cancer cells as a promising target for epigenetic therapy. Carcinogenesis 2015;36:192−201.

[23] Ghoshal A, Ghosh SS. Expression, purification, and therapeutic implications of recombinant sFRP1. Appl Biochem Biotechnol 2015; 175:2087−103.

[24] Heinrich MC, Patterson J, Beadling C, Wang Y, Debiec-Rychter M, Dewaele B, et al. Genomic aberrations in cell cycle genes predict progression of KIT-mutant gastrointestinal stromal tumors (GISTs). Clin Sarcoma Res 2019;9:3. 019-0112-7. eCollection 2019.

[25] Indio V, Astolfi A, Tarantino G, Urbini M, Patterson J, Nannini M, et al. Integrated molecular characterization of gastrointestinal stromal tumors (GIST) harboring the rare D842V mutation in PDGFRA gene. Int J Mol Sci 2018;19. https://doi.org/10.3390/ijms19030732.

[26] Saponara M, Urbini M, Astolfi A, Indio V, Ercolani G, Del Gaudio M, et al. Molecular characterization of metastatic exon 11 mutant gastrointestinal stromal tumors (GIST) beyond KIT/PDGFRalpha genotype evaluated by next generation sequencing (NGS). Oncotarget 2015;6:42243−57.

[27] Ou WB, Ni N, Zuo R, Zhuang W, Zhu M, Kyriazoglou A, et al. Cyclin D1 is a mediator of gastrointestinal stromal tumor KIT-independence. Oncogene 2019;38:6615−29.

[28] Nojima M, Suzuki H, Toyota M, Watanabe Y, Maruyama R, Sasaki S, et al. Frequent epigenetic inactivation of SFRP genes and constitutive activation of Wnt signaling in gastric cancer. Oncogene 2007;26: 4699−713.

[29] Meng Y, Wang QG, Wang JX, Zhu ST, Jiao Y, Li P, et al. Epigenetic inactivation of the SFRP1 gene in esophageal squamous cell carcinoma. Dig Dis Sci 2011;56:3195−203.

[30] Kinoshita T, Nomoto S, Kodera Y, Koike M, Fujiwara M, Nakao A. Decreased expression and aberrant hypermethylation of the SFRP genes in human gastric cancer. Hepato-Gastroenterology 2011;58: 1051−6.

[31] Davaadorj M, Imura S, Saito YU, Morine Y, Ikemoto T, Yamada S, et al. Loss of SFRP1 expression is associated with poor prognosis in hepatocellular carcinoma. Anticancer Res 2016;36: 659−64.

[32] Wang Z, Li R, He Y, Huang S. Effects of secreted frizzled-related protein 1 on proliferation, migration, invasion, and apoptosis of colorectal cancer cells. CancerCell Int 2018;18:48. 018-0543-x. eCollection 2018.

[33] Wang Z, Ye Y, Liu D, Yang X, Wang F. Hypermethylation of multiple Wnt antagonist genes in gastric neoplasia: is H pylori infection blasting fuse? Medicine 2018;97:e13734 (Baltimore).

[34] Igarashi S, Suzuki H, Niinuma T, Shimizu H, Nojima M, Iwaki H, et al. A novel correlation between LINE-1 hypomethylation and the malignancy of gastrointestinal stromal tumors. Clin Cancer Res 2010;16:5114−23.

[35] Liu X, Fu J, Bi H, Ge A, Xia T, Liu Y, et al. DNA methylation of SFRP1, SFRP2, and WIF1 and prognosis of postoperative colorectal cancer patients. BMC Canc 2019;19:1212. 019-6436-0.

[36] Feng Q, Stern JE, Hawes SE, Lu H, Jiang M, Kiviat NB. DNA methylation changes in normal liver tissues and hepatocellular carcinoma with different viral infection. Exp Mol Pathol 2010;88: 287−92.

[37] Fukui T, Kondo M, Ito G, Maeda O, Sato N, Yoshioka H, et al. Transcriptional silencing of secreted frizzled related protein 1 (SFRP 1) by promoter hypermethylation in non-small-cell lung cancer. Oncogene 2005;24:6323−7.